

## STABILITY OF SUSPENSIONS FOR ELECTRONIC APPLICATIONS

### Abstract

Many processes in the fabrication of electronic devices use suspensions at one point or another. Wafers are polished using CMP slurries, carbon nanotubes are incorporated in various materials to enhance their thermal, electrical or mechanical properties, fuel cells and flat panel displays comprise coated surfaces with nanoparticles, etc. All of these suspensions show typical colloidal instabilities (sedimentation, flocculation). Therefore, it is important to test their stability in the shortest possible time in order to improve the delay from development to production in a very competitive market. All these destabilizations can be monitored and quantified using the optical device Turbiscan<sup>®</sup>. Analyses are done on the real product, without dilution and can be automated and accelerated through temperature increase.

**Keywords:** CNT, CMP, FDP, dispersion, suspension, stability, Turbiscan<sup>®</sup>.

### Introduction

Semi-conductors, flat panel displays, multilayer capacitors, and most electronic devices which surround everyone of us in our everyday life are fabricated *via* a process where a suspension is involved. Even if these dispersions are not end-products but are used in a process, their stability is crucial for the good quality of these very high tech systems. Sedimentation and flocculation phenomena need to be tracked and quantified in order to minimize their intensity, hence getting reproducible and high quality processes.

In this paper we present various examples of stability studies using the Turbiscan<sup>®</sup> optical device.

### Experimental procedure

#### 1. Principle of the measurement

The heart of the optical scanning analyser, Turbiscan<sup>®</sup>, is a detection head, which moves up and down along a flat-bottom cylindrical glass cell (Figure 1)<sup>1-2</sup>. The detection head is composed of a pulsed near infrared light source ( $\lambda = 880 \text{ nm}$ ) and two synchronous detectors. The transmission detector (at  $180^\circ$ ) receives the light, which goes through the sample, while the backscattering detector (at  $45^\circ$ ) receives the light scattered backward by the sample. The detection head scans the entire height of the sample, acquiring transmission and backscattering data every  $40 \mu\text{m}$ . The Turbiscan LAB can be thermo-regulated from  $4$  to  $60^\circ\text{C}$  and linked to a fully automated ageing station (Turbiscan ags) for long-term stability analyses. Increasing temperature is the ideal parameter to accelerate destabilisation processes, while maintaining realistic testing conditions.

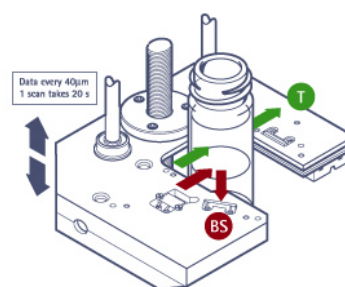


Figure 1. Principle of Turbiscan<sup>®</sup> measurement

The Turbiscan<sup>®</sup> makes scans at various pre-programmed times and overlays the profiles on one graph in order to show the destabilisation. Graphs are usually displayed in reference mode, whereby the first profile is subtracted to all other profiles, in order to enhance variations. A stable product has all the profiles overlaid on one curve (Figure 2), as an unstable formulation shows variations of the profiles (Figure 3). Backscattering and/or transmission fluxes are shown in ordinate and the height of the cell in abscissa (Figure 2 and 3). The first profile is displayed in pink, the last one in red.

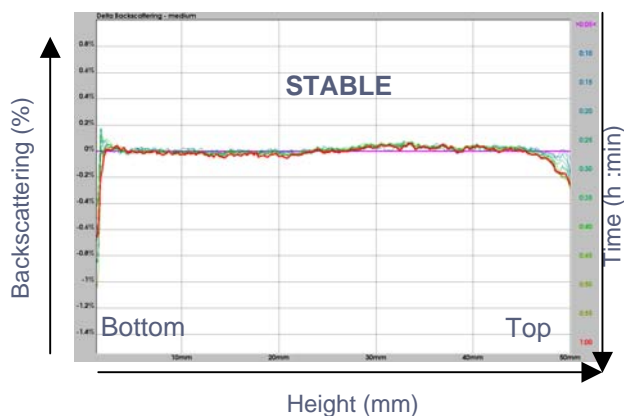


Figure 2. Superposition of scans with time for a stable sample

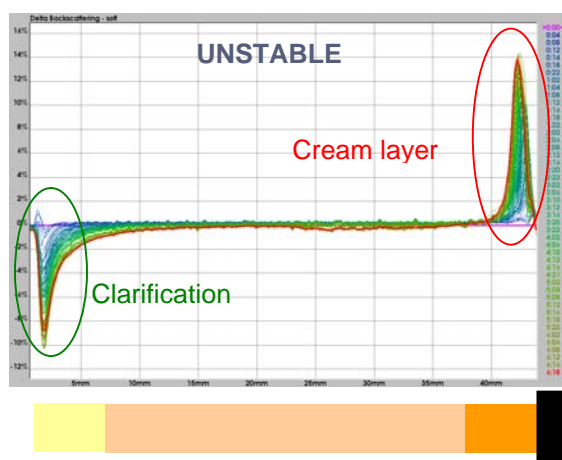


Figure 3. Superposition of scans with time for an unstable sample (creaming)

2. Instability detection

The measurement principle of the Turbiscan® range is based on multiple light scattering (MLS), where the photons are scattered many times by the particles / droplets of the dispersions before being detected by the backscattering detector. The intensity of the light backscattered by the sample depends on three parameters: the diameter of the particles, their volume fraction and the relative refractive index between the dispersed and continuous phases. Therefore, any change due to a variation of the particle size (flocculation, coalescence) or a local variation of the volume fraction (migration phenomena: creaming, sedimentation) is detected by the optical device.

a. Particle size variation

Figure 4, the variation of the backscattering level is shown as a function of the particle diameter for a fixed volume fraction of latex particles.

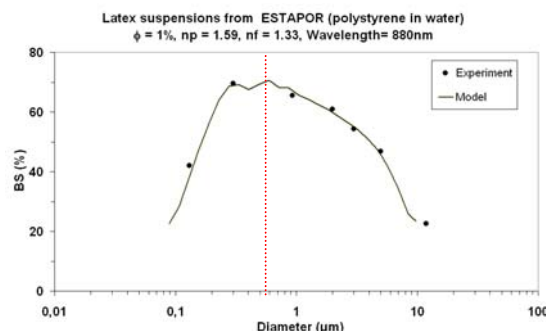


Figure 4. Backscattering level versus diameter for latex particles at 1%

The curve obtained is a bell shaped curve, where the top is linked to the wavelength of the incident light (880 nm). For particles smaller than the incident light (left part of the curve), an increase of particle size is showed by an increase in backscattering. For particles bigger than the incident light (right part of the curve), an increase in size leads to a decrease in backscattering.

On the Turbiscan® profiles, the particle size variations are displayed by a variation of the backscattering level over the total height of the sample (Figure 5).

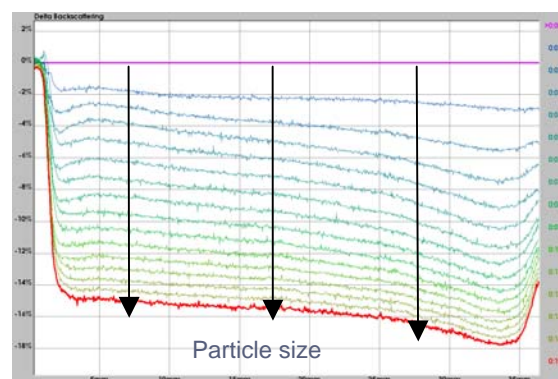


Figure 5. Typical profiles for flocculation phenomenon (initial size = 1µm)

b. Migration phenomena

Migration phenomena (sedimentation or creaming) lead to local variation of the concentration of particles in the sample.

Figure 6, the variation of transmission and backscattering levels are shown as a function of the volume fraction for a fixed diameter of latex particles.

If the concentration of particles is smaller than the critical concentration  $\phi_c$ , the product can be considered as diluted and the transmission level decreases with an increase in concentration.

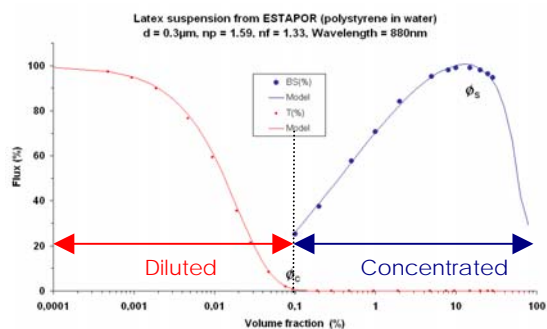


Figure 6. Transmission (red) and backscattering (blue) levels versus volume fraction for latex particles of  $0.3 \mu\text{m}$

When the concentration is sufficient ( $\phi > \phi_c$ ), there is no transmission signal (opaque product) and the backscattering level increases with an increase of the volume fraction.

When the concentration of particles becomes too high ( $\phi > \phi_s$ ), the backscattering level starts to decrease as the distance between particles is smaller than the wavelength of incident light. This phenomenon is called dependent diffusion and is mostly observed for small particles ( $< 1 \mu\text{m}$ ).

On the Turbiscan® profiles migration phenomena are displayed by local variations of the backscattering. Figure 7, the backscattering level decreases at the top (right part of the graph), due to a decrease of the concentration of particles, hence a clarification, while it increases at the bottom due to the increase of particle concentration consecutive to the sediment formation. It is interesting to note that there is no variation in the middle of the sample, indicating no particle size variation.

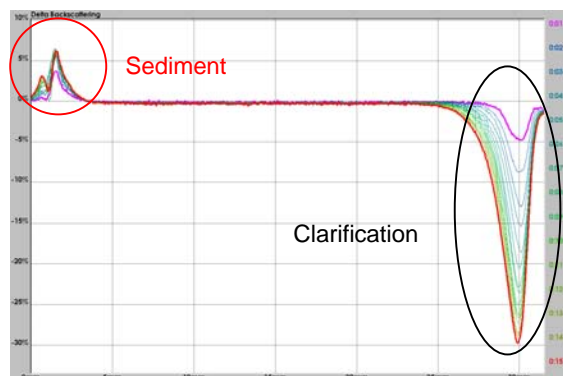


Figure 7. Typical backscattering profiles for a sedimentation phenomenon.

### 3. Materials

In this paper, various types of electronic slurries are described. For each experiment, the sample was shaken before use and 7 or 20 mL (for the Turbiscan Classic and Lab respectively) was sampled in a borosilicate glass cell. The vial is then closed with a stopper and placed in the Turbiscan®.

## Results and discussion

### 1. Stability of platinum nanoparticles for fuel cell applications

Fuel cells have been extensively studied during these last decades as they appear as environmentally friendly power sources. They convert the chemicals hydrogen and oxygen into water and electricity, *via* a reaction between fuel (on the anode side) and an oxidant (on the cathode side) in the presence of an electrolyte. The reactants flow into the cell, and the reaction products flow out of it, while the electrolyte remains within it. Fuel cells can operate virtually continuously as long as the necessary flows are maintained.

Platinum is typically used as a catalyst to facilitate the chemical reaction in polymer exchange membrane fuel cells (PEMFC). It consists of a dispersion of nanoparticles.

In this work we present three formulations of platinum nanoparticles : formulation 1 consists of 50 nm Pt nanoparticles in water ; formulation 2 contains 50 nm Pt particles dispersed in IPA ; and finally formulation 3 corresponds to 100 nm Pt/Ru (1:1 wt%) nanoparticles dispersed in IPA. All these products are black colored samples, which have been studied in the Turbiscan Lab at ambient temperature for 5 hours.

Formulation 1 displays no variation of transmission or backscattering over the 5 hours of analysis (Figure 8), hence proves to be highly stable.



Figure 8. Transmission (top) and backscattering (bottom) for formulation 1 at  $25^\circ\text{C}$ .

Formulation 2, on the other hand, is undergoing large sedimentation (Figure 9), with an important increase of the transmission signal towards the top of the sample. It is important to note that when transmission signal is greater than 0.2%, backscattering signal should be overlooked as it is affected by secondary reflections on the glass. Therefore, in this example backscattering should only be considered in the bottom part (from 0 to 6.5mm).

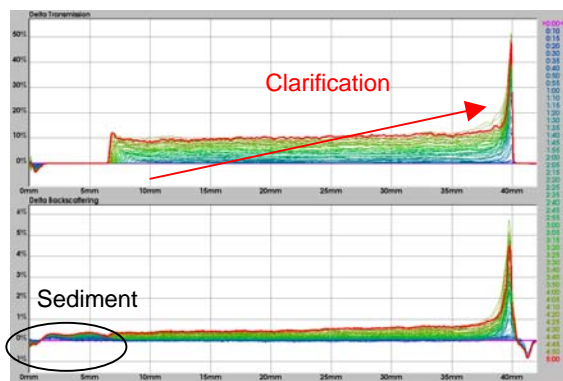


Figure 9. Delta transmission (top) and delta backscattering (bottom) for formulation 2 at 25°C.

The polarity of the solvent is therefore playing a major role in this case, in the stabilisation of the nanoparticles.

The last formulation consists of a mixture of platinum (Pt) and ruthenium (Ru) nanoparticles dispersed in IPA. Figure 10 shows that no transmission is displayed over the duration of analysis, hence no major clarification. The variation of backscattering shows an increase of the backscattering at the bottom of the vial, as the particle concentration increases due to sedimentation. At the top, a slight decrease of backscattering is seen as clarification takes place. The middle part is more peculiar, as it displays a progressive increase of the backscattering towards the bottom of the sample. This could be due to the coupling of aggregation and clarification of one of nanoparticles type, when the other type simply settles. As the nanoparticles aggregate, backscattering increases and this is emphasized by sedimentation.

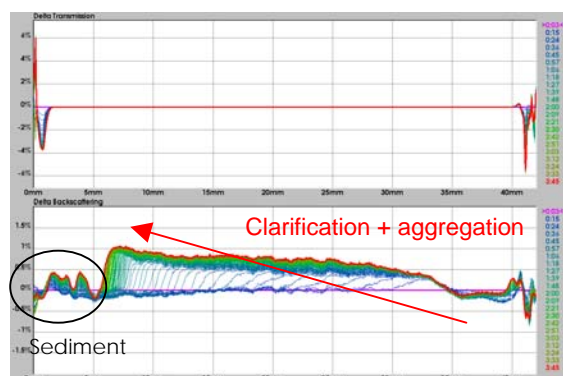


Figure 10. Delta transmission (top) and delta backscattering (bottom) for formulation 3 at 25°C.

The two populations of platinum and ruthenium nanoparticles would therefore exhibit a different behaviour. It is likely that platinum is showing only sedimentation, when looking at data from the two other formulations. Therefore the middle part would be due to the aggregation and sedimentation of ruthenium nanoparticles.

## 2. Stability of multi-walled carbon nanotubes (MWCNT)

Carbon nanotubes have attracted a vast amount of attention because of their exceptional electrical, thermal and mechanical properties. Many research groups are currently working on their incorporation in various materials to enhance their physical properties. However, one of the major issue they are facing is the difficulty to disperse them. Surface modifications and addition of surfactants or polymers are commonly used to face this problem<sup>3</sup>.

Kim *et al.*<sup>3</sup> have used the Turbiscan to monitor the effect of various surfactants on MWCNT dispersibility: NaDDBS, CTAB and Triton X-100. The concentration of each surfactant was 0.3wt% for 0.02wt% of MWCNT dispersed in water. The MWCNT were characterised by SEM and TEM giving sizes of  $1.3 \pm 0.7 \mu\text{m}$  in length and  $20 \pm 3\text{nm}$  in diameter ( $n=50$ ).

Figure 11 the mean value of transmission is computed over the total height and shows that without any surfactant (squares), the variation of transmission is large, indicating an aggregation of the particles. When surfactant is used, this aggregation is not observed and the MWCNT remains well dispersed.

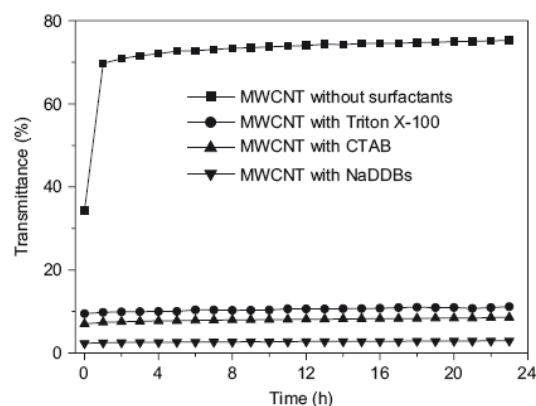


Figure 11. Mean value of transmission for MWCNT stabilised by different surfactant systems.

## 3. Stability of ceria slurry for Chemical Mechanical Polishing (CMP)

Chemical-mechanical polishing (CMP), is a technique used in semiconductor fabrication for planarizing a wafer or other substrates. The process uses an abrasive and corrosive chemical slurry in conjunction with a polishing pad and retaining ring. The abrasive accelerates this weakening process and the polishing pad helps to wipe the reacted materials from the surface. This removes material and tends to even out any irregular topography, making the wafer flat or planar at the Angstrom level.

Cerium(IV) oxide, also known as ceria, is an oxide of the rare earth metal cerium. It is known to have a high polishing efficiency for oxide film, but also it has an unfavourable reputation for problems linked to its quick sedimentation and agglomeration of

particles, which can alter significantly the CMP process, leaving unwanted defects. Therefore it is necessary to tailor the ceria slurry in order to reach the right stability requirements for CMP applications. Polymeric dispersants are typically used to stabilise ceria particles, *via* steric stabilisation. Hence, the molecular weight of the dispersant plays a key role in the stability efficiency.

We present here stability analyses of three suspensions of ceria using the Turbiscan LAB at 35°C for 12 hours. Formulation A contains high, formulation B intermediate and formulation C low molecular weight of dispersant.

All three formulations display a similar behaviour (Figure 12) with a decrease of the backscattering signal at the top as the particles deplete from this region due to a sedimentation process. Simultaneously backscattering increases at the bottom of the vial, where the particles settle. Transmission increases at the top when clarification is large enough for light to cross the suspension.

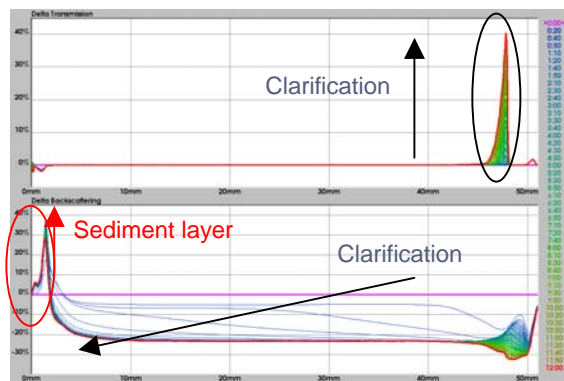


Figure 12. Delta transmission (top) and delta backscattering (bottom) for Ceria suspension A at 35°C.

In order to compare the extent of sedimentation in the three formulations; it is possible to compute the speed of clarification (table 1) from the slope of the thickness of the clarified layer (Figure 13).

Table 1. Thickness of the clarified layer after 8 hours of analysis and clarification velocity of the three ceria suspensions

Sample	Thickness layer after 8 hours (mm)	Clarification velocity (mm/h)
A	0.29	0.17
B	29.20	2.34
C	46.00	13.87

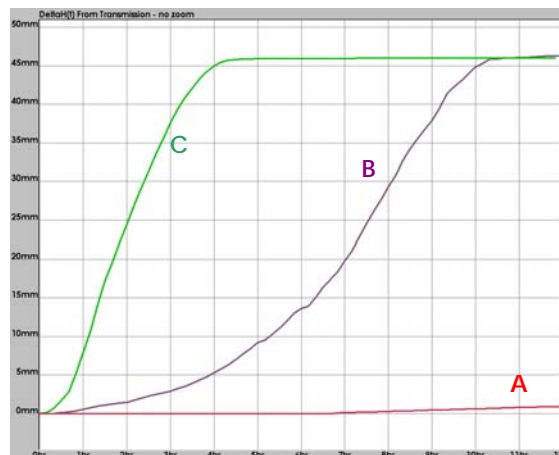


Figure 13. Thickness of clarified layer for the three ceria suspensions.

These results enable to show that at 35°C, it is possible to classify the stability against sedimentation of the ceria suspensions in a few hours. Formulation A displays the best stability and formulations C the worst. This highlights the effect of the molecular weight of polymer dispersant, where long polymer chains give rise to better steric repulsion, hence better stability.

#### 4. Ink stability for PDP process

Plasma display panel (PDP) and more generally flat panel display (FPD) are becoming a commodity in the everyday life. The xenon, neon and argon gas in a plasma television is contained in hundreds of thousands of tiny cells positioned between two plates of glass. In color panels, the back of each cell is coated with a phosphor. The ultraviolet photons emitted by the plasma excite these phosphors to give off colored light. Every pixel is made up of three separate subpixel cells, each with different colored phosphors (red, green and blue). These colors blend together to create the overall color of the pixel.

The phosphor pattern can be fabricated by several methods including ink-jet processing. This method is relatively cheap compared to others (screen printing, photolithography, etc.) and enable high productivity. However, it requires submicron-sized phosphor particles in order to avoid nozzle clogging. Kim *et al.*<sup>5</sup> present some work on synthesis of submicron spherical phosphor particles for PDP process, using reverse emulsion method. These nanoparticles of green phosphor of 200-300nm were dispersed in an aqueous solution to produce an ink, which could be further used for inkjet processing. Three formulations have been tested with different compositions (Table 2). The stability of the obtained ink was controlled using the Turbiscan LAB (Figure 15). It showed that formulation c was the most stable, which was in good correlation with size measurement (data not shown).

Table 2. Composition (wt%) of each components to fabricate phosphor ink

No.	Phosphor	H <sub>2</sub> O	BYK 192 <sup>®</sup>	SA0700 <sup>®</sup>	Acetic acid
Formulation (a)	14	66	20	0	0
Formulation (b)	14	66	0	10	10
Formulation (c)	14	66	5	7.5	7.5

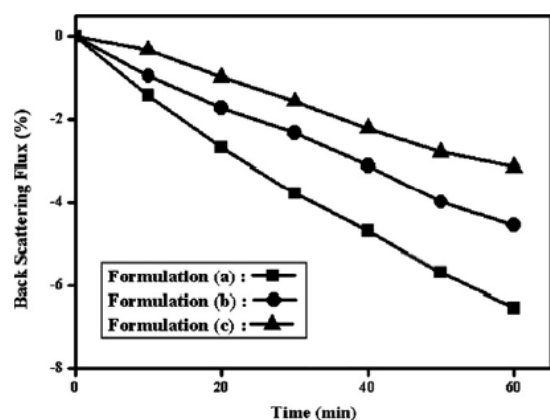


Figure 15. Mean value of backscattering the three formulation of green phosphor inks.

## Conclusion

Therefore, we have shown that the Turbiscan<sup>®</sup> is the ideal tool for identifying and quantifying destabilisation phenomena of many dispersion types, should they contain very small, highly concentrated or even colored particles, such as carbon nanotubes or CMP slurries. All the destabilisation processes can be analysed and followed separately using the different parameters available in the software. The overall stability study can be shortened from 10 to 50 times at ambient temperature. Moreover, the analyses can be accelerated even more through temperature increase. This last parameter enables to speed up destabilisation up to hundreds times, while maintaining realistic testing conditions.

## References

- Mengual, O., Meunier, G., Cayre, I., Puech, K., Snabre, P. (1999) Characterisation of instability of concentrated dispersions by a new optical analyser: the TURBISCAN MA 1000, *Colloids and Surfaces A: Physicochemical and Engineering Aspects*, 152 (1), 111-123.
- Bru, P., Brunel L., Buron H, Cayré I., Ducarre X., Fraux A., Mengual O., Meunier G., de Sainte Marie A., (2004) Particle size and rapid stability analyses of concentrated dispersions: Use of multiple light scattering, ACS Symposium series 881ed T. Provder and J. Texter, 45-60.
- Kim H-S., Park W-I., Kang M., Jin H-J (2008). Multiple light scattering measurement and stability analysis of aqueous carbon nanotube dispersions. *Journal of Physics and Chemistry of Solids*, 69 (5-6), 1209-1212.
- Hong, S., Kim, M., Hong, C.K., Jung, D., Shim, S.E. (2008) Encapsulation of multi-walled carbon nanotubes by poly(4-vinylpyridine) and its dispersion stability in various solvent media, *Synthetic Metals*, 158 (21), 900-907.
- Moon, J.S., Park, J.H., Lee, T.Y., Kim, Y.W., Yoo, J.B., Park, C.Y., Kim, J.M., Jin, K.W. (2005) Transparent conductive film based on carbon nanotubes and PEDOT composites *Diamond & Related Materials*, 14 (11), 1882-1887
- Lee J., Kim M., Hong C.K., Shim S.E. (2007) Measurement of the dispersion stability of pristine and surface-modified multiwalled carbon nanotubes in various nonpolar and polar solvents, *Measurement Science and Technology*, 18 (12), 3707-3712.
- Kim, S.H., Han, Y.S., Kwon, Y., Hur, Y., Kwak, G., Hur, B.K., Park, L.S. (2008) Synthesis of submicron-sized spherical green phosphors by reverse emulsion method and their application to phosphor inks for ink-jet process in PDP, Displays, 29 (4), 333-338.